Journal of Cerebral Blood Flow & Metabolism (2013) 33, 684–691

www.jcbfm.com

ORIGINAL ARTICLE

Glutamate metabolism is impaired in transgenic mice with tau hyperphosphorylation

Linn Hege Nilsen[1], Caroline Rae[2], Lars M Ittner[3], Jürgen Götz[3,4] and Ursula Sonnewald[1]

In neurodegenerative diseases including Alzheimer's disease and frontotemporal dementia, the protein tau is hyperphosphorylated and eventually aggregates to develop neurofibrillary tangles. Here, the consequences of tau hyperphosphorylation on both neuronal and astrocytic metabolism and amino-acid neurotransmitter homeostasis were assessed in transgenic mice expressing the pathogenic mutation P301L in the human tau gene (pR5 mice) compared with nontransgenic littermate controls. Mice were injected with the neuronal and astrocytic substrate [1-^{13}C]glucose and the astrocytic substrate [1,2-^{13}C]acetate. Hippocampus and cerebral cortex extracts were analyzed using ^{1}H and ^{13}C nuclear magnetic resonance spectroscopy, gas chromatography–mass spectrometry and high-performance liquid chromatography. The glutamate level was reduced in the hippocampus of pR5 mice, accompanied by reduced incorporation of ^{13}C label derived from [1-^{13}C]glucose in glutamate. In the cerebral cortex, glucose utilization as well as turnover of glutamate, glutamine, and GABA, were increased. This was accompanied by a relative increase in production of glutamate via the pyruvate carboxylation pathway in cortex. Overall, we revealed that astrocytes as well as glutamatergic and GABAergic neurons in the cortex of pR5 mice were in a hypermetabolic state, whereas in the hippocampus, where expression levels of mutant human tau are the highest, glutamate homeostasis was impaired.

Journal of Cerebral Blood Flow & Metabolism (2013) **33,** 684–691; doi:10.1038/jcbfm.2012.212; published online 23 January 2013

Keywords: astrocytes; dementia; GABA; glutamate; MR spectroscopy; neurotransmitters

INTRODUCTION

In the normal adult brain, the microtubule-associated protein tau is mainly localized to axons, where it has a role in the assembly and stabilization of microtubules. Tau is also the principal component of the intracellular neurofibrillary pathology that occurs in Alzheimer's disease (AD) and in tauopathies such as frontotemporal dementia (FTD) with Parkinsonism linked to chromosome 17 (FTDP-17).[1,2] In these conditions, tau is hyperphosphorylated. This compromises its ability to bind to microtubules[3] which may lead to microtubule destabilization and impairment of vital cellular processes such as axonal transport.[4,5] Tau is subsequently translocated to the somatodendritic compartment where it, with time, accumulates into filamentous aggregates and assembles into neurofibrillary tangles (NFTs).[4,6] The discovery of a range of mutations in the tau gene (microtubule-associated protein tau; MAPT) in FTDP-17 in humans has firmly established that tau dysfunction can lead to neurodegeneration and dementia,[7–10] although mutations in the tau gene have not been identified in AD.

A range of studies indicate that tau pathology is accompanied by metabolic alterations in the brain. In FTD, cerebral glucose metabolism is predominantly decreased in frontal and temporal regions and also in subcortical structures.[11–14] In AD, glucose hypometabolism is severe in the parieto-temporal, posterior cingulate and frontal cortices and the medial temporal lobes.[15] High levels of phosphorylated tau in cerebrospinal fluid have been associated with hypometabolism of glucose in patients with mild cognitive impairment (MCI),[16] and alterations in metabolite levels preceding symptoms have been demonstrated with *in vivo* ^{1}H magnetic resonance spectroscopy in *MAPT* mutation carriers.[17] The details of how tau pathology specifically affects the pathways of glucose metabolism in the brain are not well understood. Glucose is the main energy substrate of the adult mammalian brain, and is also the precursor of the principal excitatory and inhibitory neurotransmitters in the central nervous system, glutamate and GABA, respectively. Homeostasis of these neurotransmitters is also essentially dependent upon neuronal–astrocytic interactions via the glutamate/GABA–glutamine cycle.[18]

The current study was conducted to assess the effect of hyperphosphorylated tau on brain energy metabolism and amino-acid neurotransmitter homeostasis, using transgenic mice that express the FTDP-17 mutation P301L in the human tau gene. These pR5 mice accumulate hyperphosphorylated tau and eventually develop NFTs.[19,20] To specifically and simultaneously probe neuronal and astrocytic metabolism, transgenic pR5 mice and wild-type littermate controls were injected with a combination of [1-^{13}C]glucose and [1,2-^{13}C]acetate. Glucose is taken up by both neurons and astrocytes, but most of the acetyl Coenzyme A (acetyl CoA) derived from glucose is metabolized in neurons.[21,22] In contrast, acetate is metabolized in astrocytes but not neurons.[23] Thus, by simultaneous administration of ^{13}C-labeled glucose and acetate, neuronal and astrocytic metabolism

[1]Department of Neuroscience, Faculty of Medicine, Norwegian University of Science and Technology, Trondheim, Norway; [2]Neuroscience Research Australia, The University of New South Wales, Randwick, New South Wales, Australia; [3]Brain and Mind Research Institute, The University of Sydney, Camperdown, New South Wales, Australia and [4]Centre for Ageing Dementia Research (CADR), Queensland Brain Institute (QBI), The University of Queensland, St Lucia Campus (Brisbane), Queensland, Australia. Correspondence: Professor U Sonnewald, Department of Neuroscience, Faculty of Medicine, Norwegian University of Science and Technology, PO box 8905, MTFS, 7491 Trondheim, Norway.
E-mail: Ursula.sonnewald@ntnu.no
This work was supported by the Norwegian Health Association (Dementia) and the Department of Neuroscience DMF/NTNU. JG was supported by the Estate of Dr Clem Jones AO and by grants from the Australian Research Council and the National Health and Medical Research Council of Australia (#630516).
Received 14 November 2012; revised 10 December 2012; accepted 12 December 2012; published online 23 January 2013

can be studied in the same animal.[24] This was followed by ^{1}H and ^{13}C nuclear magnetic resonance spectroscopy (NMRS), high-performance liquid chromatography (HPLC) and gas chromatography–mass spectrometry (GC–MS) measurements of tissue extracts of cerebral cortex and hippocampus, allowing detailed mapping of the activity of metabolic pathways by analysis of the concentrations and ^{13}C labeling of metabolites.

MATERIALS AND METHODS

Materials

[1-^{13}C]Glucose and [1,2-^{13}C]acetate were purchased from Cambridge Isotope Laboratories (Andover, MA, USA), D_2O (99.9%) from CDN Isotopes (Pointe-Claire, Quebec, Canada), ethylene glycol from Merck (Darmstadt, Germany) and 2,2-Dimethyl-2-silapentane-5-sulfonate sodium salt (DSS sodium salt) from Sigma-Aldrich (St Louis, MO, USA). All other chemicals were of the purest grade available from local commercial suppliers.

Transgenic Mice

The P301L model (pR5 line) was used, in which mice express the human FTDP-17-causing P301L mutation in the longest human tau isoform; human tau40 with four microtubule-binding repeats, under control of the neuron-specific murine Thy1.2 promoter.[19] Three months old mice were chosen for the present study since this age is a pretangle stage[20] in which the consequences of tau hyperphosphorylation can be investigated in the absence of NFTs. Experiments were approved by the UNSW Animal Care and Ethics Committee (ACEC) and animals were treated in compliance with the European Convention (ETS 123 of 1986).

Intraperitoneal Injections and Tissue Extraction

Ten P301L expressing mice (pR5 tg/wt, three females and seven males) and nine control wild-type (pR5 wt/wt, two females and seven males) littermates which did not differ significantly in weight (controls 24.4 ± 1.6 g, pR5 25.7 ± 1.6 g, $P = 0.8$) were injected intraperitoneally with [1-^{13}C]glucose (543 mg/kg, 0.3 M solution) plus [1,2-^{13}C]acetate (504 mg/kg, 0.6 M solution). The mice were injected in random order. Comparable bolus injection of glucose leads to blood glucose levels well within the normoglycemic range (8.8 ± 0.5 mmol/L[22]). 15 minutes after injection, the mice were euthanized by cervical dislocation, decapitated and the brains were removed. Cerebral cortices and hippocampi were rapidly dissected and immediately immersed in liquid nitrogen. Enzyme activity was inhibited using 800 W microwave irradiation followed by extraction.

Samples were homogenized in 1 mL perchloric acid (0.7%) using a Vibra Cell sonicator (Model VCX 750, Sonics & Materials, Newtown, CT, USA), and α-ABA was added as an internal standard for HPLC analysis. Homogenized tissue samples were centrifuged at 3,000 *g* at 4 °C for 5 minutes. The pH of the supernatants was adjusted to 6.5–7.5 with KOH (0.5 M), and potassium perchlorate was removed with centrifugation. The samples were kept on ice at all times possible during the extraction procedure. After extraction, samples were lyophilized and resuspended in 200 μL D_2O, and 5 μL were removed for HPLC analysis. The samples were then twice redissolved in D_2O, frozen and lyophilized.

To assess the effect of hyperphosphorylated tau on brain energy metabolism and amino-acid neurotransmitter homeostasis, concentrations of metabolites and incorporation of ^{13}C label into metabolites in cortical extracts obtained from P301L tau transgenic pR5 mice and wild-type littermate controls were analyzed using ^{1}H and ^{13}C NMRS. Due to the small size of the hippocampus in mice, the concentrations of metabolites in hippocampus were quantified using HPLC and the distribution of ^{13}C-labeled mass isotopomers was assessed using GC–MS.

^{1}H and ^{13}C Nuclear Magnetic Resonance Spectroscopy

Lyophilized samples were dissolved in 120 μl D_2O containing 0.091 g/L DSS and 0.1% ethylene glycol as internal standards for quantification, and pH was readjusted to 6.5–7.5 with KOH. The supernatants were transferred to SampleJet tubes (3.0×103.5 mm^2) for insertion into the SampleJet autosampler (Bruker BioSpin GmbH, Rheinstetten, Germany). All samples were analyzed using a QCI CryoProbe 600 MHz ultrashielded Plus magnet (Bruker BioSpin GmbH). ^{1}H NMR spectra were acquired with the following parameters: pulse angle of 90°, acquisition time of 2.66 seconds and a relaxation delay of 10 seconds. The number of scans was 256. Proton decoupled ^{13}C NMR spectra were acquired with the following parameters: pulse angle of 30°, acquisition time of 1.65 seconds and a relaxation delay of 0.5 seconds, 30 kHz spectral width with 98 K data points. The number of scans was between 20,000 to 40,000, adjusted to the weight of the sample to achieve an appropriate signal to noise ratio. All spectra were recorded at 20 °C.

Relevant peaks in the spectra were identified and integrated using TopSpin 3.0 software (Bruker BioSpin GmbH). The amounts were quantified from the integrals of the peak areas using DSS and ethylene glycol as internal standards for the ^{1}H and ^{13}C spectra, respectively. The amounts obtained from the ^{1}H spectra were corrected for the number of protons constituting the peak and for ^{13}C content. ^{13}C-labeled metabolites were corrected for nuclear Overhauser and relaxation effects, and singlets in the ^{13}C spectra were corrected for 1.1% natural abundance of ^{13}C calculated from ^{1}H spectra. All amounts were corrected for tissue weight.

High-Performance Liquid Chromatography

HPLC (1100 series; Agilent Technologies, Santa Clara, CA, USA) with fluorescence detection was used to quantify amino-acid concentrations in the hippocampus. Amino acids were precolumn derivatized with o-phthaldialdehyde, and components were separated on a Zorbax SB-C18 column (4.6×150 mm^2, 3.5-micron; Agilent Technologies). A gradient of two eluents (one of phosphate buffer (50 mM, pH 5.9) and THF (2.5%), and the other of methanol (98.75%) and THF (1.25%)) was used to achieve optimal separation and faster elution of the nonpolar analytes. Quantification was performed using a-ABA as an internal standard. All concentrations were corrected for tissue weight.

Gas Chromatography–Mass Spectrometry

The percentage ^{13}C enrichment of metabolites in hippocampus was determined using GC–MS. Aliquots of the samples were dissolved and adjusted to pH <2 using HCl, followed by lyophilization. Amino acids and organic acids were extracted into an organic phase of ethanol and benzene, dried under air and redissolved in *N*,*N*-dimethylformamide before derivatization with MTBSTFA (*N*-Methyl-*N*-(t-Butyldimethylsilyl)trifluoroacetamide) in the presence of 1% t-butyldimethylchlorosilane. The samples were analyzed with an Agilent 6890N gas chromatograph linked to an Agilent 5975B mass spectrometer with an electron ionization source (both from Agilent Technologies). The results were corrected for natural abundance of ^{13}C using standard solutions that were run concurrently with the samples.

Interpretation of ^{13}C Labeling Patterns

The interpretation of ^{13}C labeling patterns from ^{13}C NMRS or GC–MS analyses is based on detailed knowledge of the metabolic fate of the ^{13}C-labeled compounds in neurons and astrocytes (Figure 1). A simplified view is that label from [1-^{13}C]glucose gives rise to single-labeled metabolites, whereas double-labeled metabolites are mostly derived from [1,2-^{13}C]acetate and thus astrocytic metabolism.[25]

[1-^{13}C]Glucose is via glycolysis converted to [3-^{13}C]pyruvate, which can be reduced to [3-^{13}C]lactate, transaminated to [3-^{13}C]alanine, carboxylated to oxaloacetate (OAA) in astrocytes, or decarboxylated to [2-^{13}C]acetyl CoA and subsequently enter the tricarboxylic acid (TCA) cycle. After several steps, [4-^{13}C]α-ketoglutarate (α-KG) is formed and is a precursor for [4-^{13}C]glutamate, which can subsequently be converted to [2-^{13}C]GABA in GABAergic neurons via the enzyme glutamic acid decarboxylase or to [4-^{13}C]glutamine in astrocytes via the astrocyte-specific enzyme glutamine synthetase. When [4-^{13}C]glutamate is released from glutamatergic neurons during neurotransmission, astrocytes terminate the signal by removing [4-^{13}C]glutamate from the synaptic cleft via transporters, followed by conversion to [4-^{13}C]glutamine or to [4-^{13}C]α-KG. Via the TCA cycle, [4-^{13}C]α-KG also gives rise to [2-^{13}C]-/[3-^{13}C]OAA, which can be transaminated to [2-^{13}C]-/[3-^{13}C]aspartate. From the second turn of the TCA cycle, [2-^{13}C]-/[3-^{13}C]glutamate and glutamine and [4-^{13}C]-/[3-^{13}C]GABA can be formed after several steps if OAA labeled from the first turn of the cycle condenses with unlabeled acetyl CoA. [2-^{13}C]glutamate is also formed as a result of pyruvate carboxylation in astrocytes. It should be noted that if OAA labeled from the first turn of the TCA cycle condenses with labeled acetyl CoA, double-labeled isotopomers of glutamate and GABA can be formed from neuronal metabolism as well.

[1,2-^{13}C]Acetate is converted to [1,2-^{13}C]acetyl CoA in astrocytes. Following entry into the TCA cycle, [4,5-^{13}C]α-KG is formed after several steps, and is the precursor for [4,5-^{13}C]glutamate and [4,5-^{13}C]glutamine. After transfer of [4,5-^{13}C]glutamine to the neuronal compartment it is

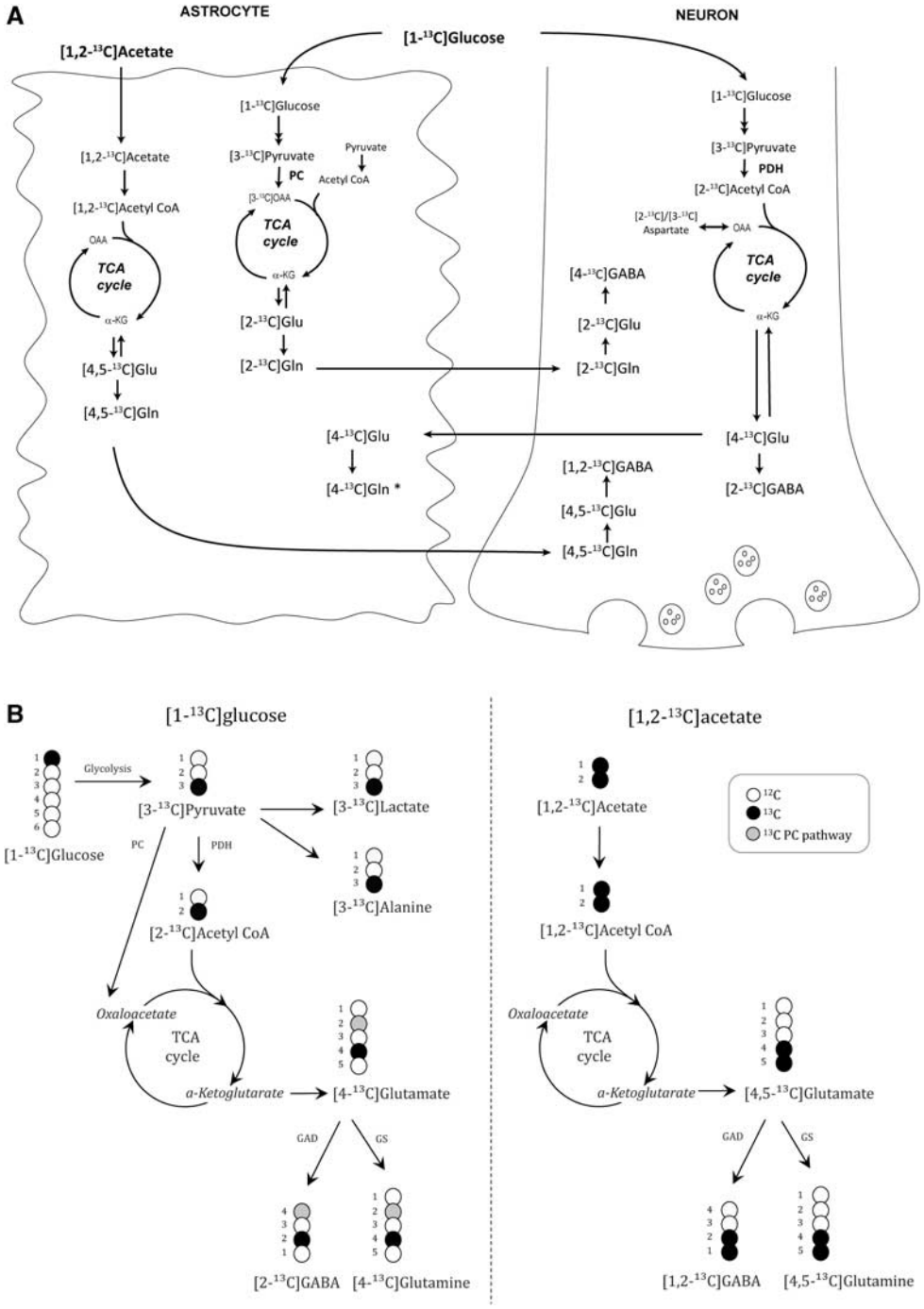

Figure 1. (**A**) A simplified overview of a selection of ^{13}C labeling patterns originating from pathways of metabolism of [1-^{13}C]glucose and [1,2-^{13}C]acetate. For simplicity, a hypothetical pluripotent neuron is represented that is both glutamatergic and GABAergic. [1-^{13}C]Glucose is converted to [3-^{13}C]pyruvate via glycolysis, and [3-^{13}C]pyruvate can be decarboxylated to [2-^{13}C]acetyl CoA and subsequently enter the TCA cycle. After several steps, [4-^{13}C]α-KG is formed and is precursor for [4-^{13}C]glutamate, which can subsequently be converted to [2-^{13}C]GABA in GABAergic neurons. When [4-^{13}C]glutamate is released during neurotransmission, astrocytes take up [4-^{13}C]glutamate from the synaptic cleft and convert it to [4-^{13}C]glutamine. In astrocytes, [3-^{13}C]pyruvate originating from [1-^{13}C]glucose can also be converted to [3-^{13}C]OAA by the action of pyruvate carboxylase and give rise to [2-^{13}C]glutamate after several steps. This can be converted to [2-^{13}C]glutamine and sent to neurons for conversion to [2-^{13}C]glutamate and to [4-^{13}C]GABA in GABAergic neurons. [1,2-^{13}C]Acetate is converted to [1,2-^{13}C]acetyl CoA in astrocytes. Following entry into the TCA cycle, [4,5-^{13}C]α-KG is formed after several steps, and is the precursor for [4,5-^{13}C]glutamate and [4,5-^{13}C]glutamine. After transfer of [4,5-^{13}C]glutamine to the neuronal compartment, it is reconverted to [4,5-^{13}C]glutamate in glutamatergic neurons and further to [1,2-^{13}C]GABA in GABAergic neurons. *It should be noted that [4-^{13}C]glutamine can be synthesised from [1-^{13}C]glucose in astrocytes as well, but this is omitted from the figure for simplicity. (**B**) Schematic representation of glutamate, glutamine and GABA isotopomers derived from [1-^{13}C]glucose and [1,2-^{13}C]acetate. Black circles represent ^{13}C labeling, white circles represent ^{12}C, and gray circles indicates labeling of metabolites from pyruvate carboxylation. For more details, see the Materials and methods section. α-KG, α-ketoglutarate; acetyl CoA, acetyl Coenzyme A; GAD, glutamic acid decarboxylase; Glu, glutamate; Gln, glutamine; GS, glutamine synthetase; OAA, oxaloacetate; PC, pyruvate carboxylase; PDH, pyruvate dehydrogenase; TCA, tricarboxylic acid cycle.

reconverted to [4,5-^{13}C]glutamate in glutamatergic neurons, which can be converted to [1,2-^{13}C]GABA in GABAergic neurons. If [4,5-^{13}C]α-KG is metabolized in the TCA cycle, it may give rise to formation of [3-^{13}C]-/[1,2-^{13}C]glutamate and glutamine and [3-^{13}C]-/[4-^{13}C]GABA from the second turn of the cycle if labeled OAA condenses with unlabeled acetyl CoA.

Using mass spectrometry, the percentage of the metabolite with one (M + 1) or several (M + x) ^{13}C atoms is detected, but the exact positions of the ^{13}C atoms in the molecule are not revealed. Thus, GC–MS results represent the sum of all different positional isotopomers of a metabolite with the same number of labeled carbon atoms. The majority of M + 1 glutamate consists of [4-^{13}C]glutamate, that of M + 1 glutamine is [4-^{13}C]glutamine, that of M + 1 GABA is [2-^{13}C]GABA, that of M + 1 aspartate is [2-^{13}C]- and [3-^{13}C]aspartate, whereas that of M + 1 lactate is [3-^{13}C]lactate. The majority of M + 2 glutamate is [4,5-^{13}C]glutamate, that of M + 2 glutamine is [4,5-^{13}C]glutamine, whereas that of M + 2 GABA is [1,2-^{13}C]GABA. M + 2 metabolites thus primarily represent metabolites derived from astrocytic metabolism.

Calculation of relative contributions from different metabolic pathways (metabolite ratios). Because calculation of metabolite ratios requires distinction between positional isotopomers, they could only be calculated for the cerebral cortex.

Pyruvate can be converted by pyruvate dehydrogenase (PDH) to acetyl CoA or by pyruvate carboxylase (PC) to OAA, and this will give rise to differently ^{13}C-labeled glutamate, glutamine and GABA. The contribution of the anaplerotic (PC) versus the oxidative pathway (PDH) to formation of glutamate, glutamine and GABA can thus be calculated from the ratios of these isotopomers.[24] In astrocytes, [3-^{13}C]pyruvate formed from [1-^{13}C]glucose can give rise to [3-^{13}C]OAA via the astrocyte-specific enzyme PC. This may subsequently give rise to formation of [2-^{13}C]glutamate and [2-^{13}C]glutamine. The latter can be transported to neurons and be reconverted to [2-^{13}C]glutamate and subsequently to [4-^{13}C]GABA in GABAergic neurons. However, [2-^{13}C]glutamate or glutamine can also be formed from the second turn of the TCA cycle in equal amounts as [3-^{13}C]glutamate or glutamine due to scrambling of the ^{13}C label in the symmetrical succinate/fumarate steps. [3-^{13}C]Glutamate or glutamine can also be derived from the second turn of the TCA cycle during [1,2-^{13}C]acetate metabolism, in equal amounts as [1,2-^{13}C]glutamate or glutamine. Therefore, [2-^{13}C]glutamate or glutamine in excess of [3-^{13}C]glutamate or glutamine corrected for the contribution labeled from acetate arises from PC activity. The ratio for glutamate and glutamine is calculated as follows: ([2-^{13}C]–([3-^{13}C]–[1,2-^{13}C]))/[4-^{13}C]. We also calculated the ratios for cycling and acetate/glucose utilization as described by Kondziella *et al*.[26]

Data and Statistical Analysis

Due to experimental errors, the numbers of samples for each group varied. One cerebral cortex sample from a control mouse was lost during the experiment, and one pR5 mouse was not injected properly and was discarded from all data sets. In addition, it was not possible to obtain adequate ^{13}C NMRS or GC–MS spectra of one pR5 cerebral cortex sample and one control cerebral cortex and hippocampus sample. These were not included in the ^{13}C-related data sets. Percentage enrichment of metabolites in cortex was calculated as the ^{13}C amount divided by the total concentration of the metabolite (^{12}C + ^{13}C) and expressed as a percentage. Mass isotopomers for cortex were calculated as the sum of all single- or double-labeled isotopomers of a metabolite detected with ^{13}C NMRS as a percentage of the concentration detected with ^{1}H NMRS. It should be noted that for both calculations, single-labeled metabolites were corrected for natural abundance of ^{13}C.

All results are presented as average ± s.e.m. Statistical differences between the control and pR5 group were assessed using the two-tailed Student's *t*-test with $P < 0.05$ as the level of significance (not corrected for multiple comparisons).

RESULTS

Concentrations of Metabolites

We measured the concentrations of metabolites in cerebral cortex using ^{1}H NMRS and in hippocampus using HPLC. The use of different methods yielded slightly different sets of metabolites for the two brain areas. For the cerebral cortex these were: NADH, fumarate, myo-inositol, phosphocreatine, creatine, glycine, taurine, glycerophosphocholine, phosphocholine, choline, aspartate, glutamine, glutamate, GABA, *N*-acetylaspartate, alanine, and lactate. For the hippocampus these were: glutamate, glutamine, GABA, aspartate, glutathione, serine, glycine, threonine, arginine, taurine, alanine, tyrosine, lysine, methionine, tryptophan, valine, phenylalanine, isoleucine, and leucine. The only significant difference in metabolite levels between the two groups was in that of hippocampal glutamate, which was decreased in pR5 mice (Only the concentrations of glutamate, glutamine, aspartate and GABA are shown; Table 1).

[1-^{13}C]Glucose and [1,2-^{13}C]Acetate Metabolism in Cortex

The concentration of [1-^{13}C]glucose was significantly decreased in the cortex of pR5 mice (46.3 ± 5.1 nmol/g in controls and 31.7 ± 4.1 nmol/g in pR5 mice, $P = 0.049$). The percentage enrichment of [4-^{13}C]glutamate and [4-^{13}C]glutamine were significantly increased in pR5 mice compared with controls, whereas that of [2-^{13}C]GABA remained unchanged (Figure 2A). The percentage enrichment of [2-^{13}C]- and [3-^{13}C]glutamate and glutamine were significantly increased in pR5 mice, as was [3-^{13}C]- and [4-^{13}C]GABA (Table 2). The percentage enrichment of [3-^{13}C]lactate, [3-^{13}C]alanine and [3-^{13}C]aspartate remained unaltered in pR5 mice (as [2-^{13}C]aspartate is formed in equal amounts, only [3-^{13}C]aspartate is presented). Calculated percentage enrichments of M + 1 glutamate, glutamine, and GABA were significantly increased in pR5 mice, whereas those of M + 1 lactate and aspartate remained unchanged (Table 3).

Reflecting astrocytic metabolism, the percentage enrichment of [4,5-^{13}C]glutamate, [4,5-^{13}C]glutamine and [1,2-^{13}C]GABA were significantly increased in the cerebral cortex of pR5 mice compared with controls (Figure 2B). Calculation of M + 2 isotopomers from NMRS results demonstrated that the percentage enrichment of M + 2 glutamate and glutamine were increased, whereas that of M + 2 GABA remained unaltered (Table 3).

Metabolite ratios. The PC/PDH ratio for glutamate was significantly increased in pR5 mice compared with controls (controls 0.07 ± 0.01 and pR5 0.13 ± 0.02, $P = 0.015$), but was unaltered for glutamine (results not shown). Acetate/glucose utilization and cycling ratios remained unchanged (results not shown).

[1-^{13}C]Glucose and [1,2-^{13}C]Acetate Metabolism in Hippocampus

The percentage enrichment of M + 1 glutamate, glutamine, GABA, and aspartate were unchanged in the hippocampus of pR5 mice compared with controls (Table 3). Unaltered M + 1 glutamate

Table 1. Metabolite concentrations in cerebral cortex and hippocampus

	Cerebral cortex (μmol/g tissue)[a]		*Hippocampus (μmol/g tissue)*[b]	
	Control	*pR5*	*Control*	*pR5*
Glutamate	10.0 ± 0.6	9.2 ± 0.3	13.9 ± 0.9	10.7 ± 1.0*
Glutamine	6.7 ± 0.8	5.6 ± 0.7	9.7 ± 1.5	7.3 ± 1.3
GABA	3.5 ± 0.1	3.3 ± 0.3	4.4 ± 0.4	6.1 ± 1.1
Aspartate	3.9 ± 0.2	3.7 ± 0.3	4.8 ± 0.5	6.0 ± 1.0

The concentrations of glutamate, glutamine, GABA, and aspartate in cerebral cortex and hippocampus. Results are presented as average ± s.e.m. in μmol/g brain tissue in control ($n = 7$ for cerebral cortex and $n = 8$ for hippocampus) and pR5 mice ($n = 9$). *$P = 0.028$, statistically significant difference between control and pR5 mice calculated using the Student's *t* test. [a]Concentrations were measured using ^{1}H NMR spectroscopy. [b]Concentrations were measured using high-performance liquid chromatography.

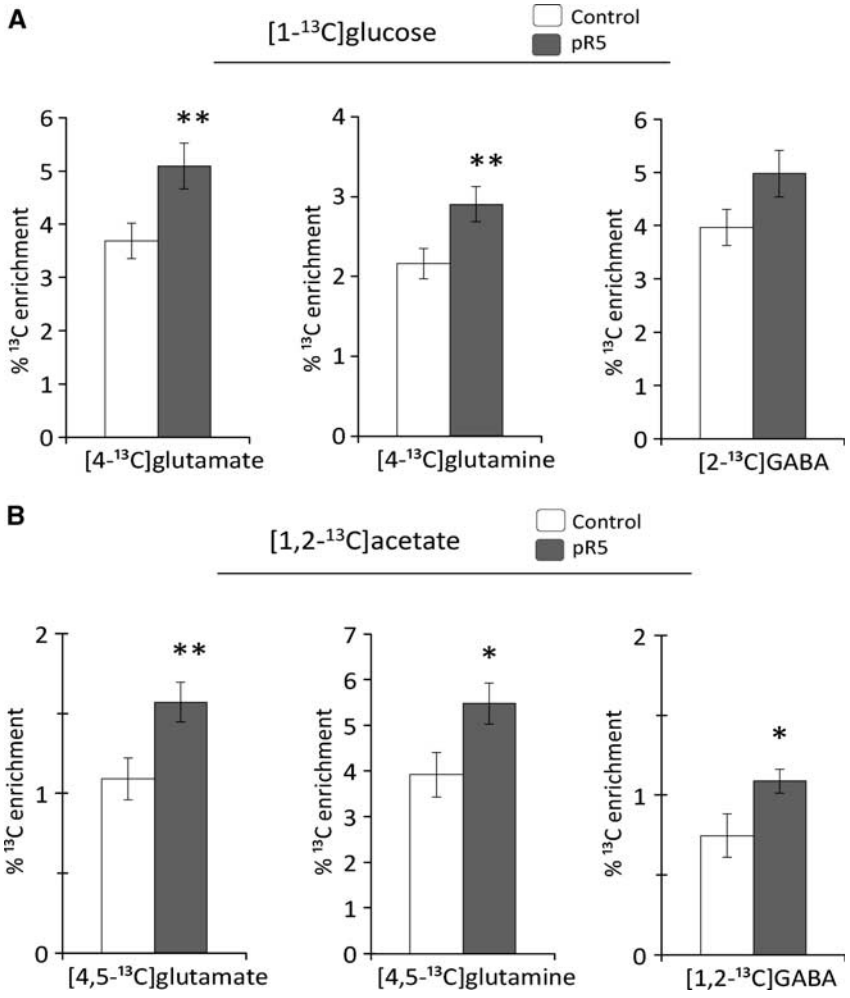

Figure 2. The amount of [4,5-^{13}C]glutamate and glutamine, [4-^{13}C]glutamate and glutamine, [1,2-^{13}C]GABA and [2-^{13}C]GABA as percentage of the glutamate, glutamine, and GABA content (percentage ^{13}C enrichment) in the cerebral cortex. These isotopomers are derived from metabolism of (**A**) [1-^{13}C]glucose and (**B**) [1,2-^{13}C]acetate. Results are presented as average ± s.e.m. in control ($n = 7$, white bars) and pR5 ($n = 8$, gray bars) mice. *$P < 0.04$, **$P \leqslant 0.025$, statistically significant difference between control and pR5 mice calculated using Student's *t* test.

Table 2. The percentage ^{13}C enrichment of metabolites in cerebral cortex

	Cerebral cortex		
	Control	*pR5*	P *value*
[3-^{13}C]lactate	3.9 ± 0.4	5.0 ± 0.5	0.117
[3-^{13}C]alanine	3.5 ± 0.4	4.3 ± 0.6	0.315
[2-^{13}C]glutamate	1.1 ± 0.2	1.9 ± 0.1**	0.006
[3-^{13}C]glutamate	1.2 ± 0.2	1.7 ± 0.1*	0.014
[2-^{13}C]glutamine	0.8 ± 0.2	1.5 ± 0.2**	0.007
[3-^{13}C]glutamine	1.5 ± 0.2	2.2 ± 0.2*	0.029
[3-^{13}C]GABA	1.7 ± 0.2	2.3 ± 0.2*	0.043
[4-^{13}C]GABA	1.7 ± 0.3	2.6 ± 0.3*	0.032
[3-^{13}C]aspartate	2.2 ± 0.2	2.9 ± 0.3	0.102

The percentage ^{13}C enrichment of metabolites in the cerebral cortex of control ($n = 7$) and pR5 ($n = 8$) mice. Results are presented as average ± s.e.m. The mice were injected with [1-^{13}C]glucose and [1,2-^{13}C]acetate, for details see Materials and Methods. *$P < 0.05$. **$P < 0.01$, statistically significant difference between control and pR5 mice calculated using the Student's *t* test.

signifies that the amount of single-labeled ^{13}C glutamate was decreased proportionally to the total concentration of glutamate in the hippocampus.

The percentage enrichment of M + 2 glutamate was significantly increased in pR5 mice, but all other M + 2 metabolites remained unchanged (Table 3). In light of the decreased hippocampal glutamate level in pR5 mice, the increased M + 2 glutamate indicates that the amount of glutamate labeled from [1,2-^{13}C]acetate metabolism and thus astrocytic metabolism was either unchanged or increased. To clarify this, we calculated the amount (nmol/g) of double-labeled glutamate in the hippocampus based on the glutamate content from HPLC and the percentage enrichment of M + 2 glutamate from GC–MS for each mouse. This calculation showed that there was no significant difference between the groups in the amount of double-labeled glutamate (controls 305 ± 43 nmol/g, pR5 302 ± 25 nmol/g, $P = 0.76$).

It should be noted that the level of significance was not adjusted for multiple testing, thus all results should be interpreted with care.

DISCUSSION

A range of mutant tau-expressing animal models with NFTs and memory impairment are available.[27] At the age of 3 months, P301L expressing pR5 mice already display high levels of hyperphosphorylated human tau in both axonal and somatodendritic compartments of cortical and hippocampal

Table 3. The percentage ^{13}C enrichment of metabolites in cerebral cortex and hippocampus

	Cerebral cortex[a]			*Hippocampus*[b]		
	Control	*pR5*	P *value*	*Control*	*pR5*	P *value*
Glutamate M + 1	6.0 ± 0.7	8.7 ± 0.7[c]	0.014	6.7 ± 0.6	7.7 ± 0.6	0.259
Glutamate M + 2	2.0 ± 0.3	3.0 ± 0.3[c]	0.017	2.1 ± 0.3	3.0 ± 0.3[c]	0.041
Glutamine M + 1	4.4 ± 0.5	6.6 ± 0.5[c]	0.013	4.5 ± 0.5	5.5 ± 0.5	0.149
Glutamine M + 2	4.7 ± 0.7	6.8 ± 0.6[c]	0.033	5.2 ± 0.8	6.6 ± 0.5	0.144
GABA M + 1	7.0 ± 0.6	9.6 ± 0.8[c]	0.022	7.3 ± 1.3	9.5 ± 0.6	0.124
GABA M + 2	1.0 ± 0.3	1.5 ± 0.2	0.362	2.0 ± 0.4	2.9 ± 0.3	0.065
Aspartate M + 1	3.9 ± 0.5	5.3 ± 0.5	0.066	4.9 ± 0.4	5.8 ± 0.7	0.898
Lactate M + 1	3.9 ± 0.4	5.0 ± 0.5	0.111	4.9 ± 0.4	6.2 ± 0.4[c]	0.045

The percentage of the total concentration of metabolites labeled with ^{13}C in one (M + 1) or two (M + 2) carbon atoms of the molecule. Mice were injected with [1-^{13}C]glucose and [1,2-^{13}C]acetate, for details see Materials and Methods. The results are presented as average ± s.e.m. [a]Calculated from MRS results, $n = 7$ controls and 8 pR5 mice. [b]Detected by gas chromatography - mass spectrometry, $n = 8$ controls and 9 pR5 mice. [c]Statistically significant difference between control and pR5 mice calculated using Student's *t* test.

neurons.[19,20] Neuronal and astrocytic metabolism was assessed in the cortex and hippocampus, two areas with prominent tau pathology in pR5 mice, after i.p. injection of ^{13}C-labeled glucose and acetate. It has been established that although the serum glucose level increased after i.v. bolus injection of glucose, the concentration of glucose in the brain was not affected.[22] Thus, ^{13}C labeling in metabolites reported here reflects ^{13}C enrichment in brain and not blood glucose. In the present study, we found a decreased glutamate level in hippocampus whereas in cortex, glucose utilization and turnover of glutamate, glutamine, and GABA were increased.

Decreased Glutamate Level in Hippocampus

The substantial decrease in the glutamate concentration and the proportionally decreased amount of ^{13}C-labeled glutamate (unchanged percentage enrichment) from [1-^{13}C]glucose metabolism demonstrate disrupted glutamate homeostasis in hippocampus of pR5 mice. This may occur as a consequence of reduced glucose metabolism, which indeed is found in the temporal lobe in FTD and in the hippocampus in MCI and AD patients.[13,14,28] However, we also observed an increase in percentage enrichment of lactate labeled from [1-^{13}C]glucose, indicating that turnover of lactate and thus anaerobic glycolysis was increased. This could fit well with the finding that there was downregulation of cytosolic malate dehydrogenase (cMDH) protein in these mice at the age of 8.5 months.[29] A defect in the transfer of reducing equivalents from the cytosol to mitochondria via the malate-aspartate shuttle, in which cMDH plays a prominent role, may enhance lactate production from pyruvate and lead to decreased incorporation of ^{13}C-label into the TCA cycle metabolites and those derived from mitochondrial metabolism. Using *in vivo* ^{1}H MRS, it has been shown that the level of glutamate + glutamine (Glx) is decreased in the frontal lobe of FTD patients.[30] Hippocampal glutamate levels are decreased in both animal models of AD and in AD patients, and is also reduced before plaque accumulation in transgenic AD rats.[31–33] The results of the present study demonstrate that disrupted glutamate homeostasis may also occur as a consequence of tau hyperphosphorylation before NFTs form. The apparent metabolic dysfunction as a consequence of tau pathology lends support to the hypothesis that abnormally phosphorylated tau is detrimental for neuronal function.[34,35]

Increased Turnover of Metabolites in Cortical Neurons and Astrocytes

In contrast to the decrease in glucose utilization demonstrated in FTD patients,[14] the decreased concentration of [1-^{13}C]glucose in cortex suggests that glucose utilization was increased in pR5 mice.[36] In addition, the almost universal increase in the ^{13}C enrichment of glutamate and GABA isotopomers labeled from [1-^{13}C]glucose suggests that turnover of these metabolites is increased in cortical glutamatergic and GABAergic neurons in pR5 mice. This encompasses an increased rate of synthesis since more ^{13}C label was incorporated, accompanied by a similarly increased rate of degradation of unlabeled metabolites since the overall concentration was maintained at the same level as in controls. Concerning increased turnover of [1-^{13}C]glucose metabolism in GABAergic neurons, it is interesting to note that the percentage enrichment of [2-^{13}C]GABA was not significantly different between the groups, but there was a clear tendency towards an increase in pR5 mice. However, this lack of a significant difference was most likely caused by the unfortunate large variation in the data obtained. The concomitant increases in glutamine labeled from [1-^{13}C]glucose and [1,2-^{13}C]acetate strongly indicate enhanced turnover of glutamine in cortical astrocytes in pR5 mice. Whereas [4,5-^{13}C]glutamine is only labeled via astrocytic metabolism, 40% of [4-^{13}C]glutamine is derived from [4-^{13}C]glutamate initially labeled in the neuronal compartment.[37] Thus, the major part of [4-^{13}C]glutamine is derived from astrocytic metabolism of [1-^{13}C]glucose, but a substantial fraction reflects neuronal metabolism of [1-^{13}C]glucose and the transfer of glutamate to astrocytes. The increased percentage enrichment of [4-^{13}C]glutamine in the present study is probably a result of both the increased turnover of glutamate in the neuronal compartment and increased turnover of glutamine in astrocytes. Interestingly, the increased PC/PDH ratio for glutamate in pR5 mice suggests an increased relative contribution of the PC pathway in astrocytes to glutamate synthesis. If this is due to increased PC activity, it might present a reason why glutamate is maintained at the normal level in the cortex of pR5 mice, whereas it was decreased in the hippocampus.

The transfer of metabolites between neurons and astrocytes in cortex appeared to remain normal. This was indicated by the increase in percentage enrichment of both [4-^{13}C] glutamate and glutamine (which can suggest normal transfer of glutamate from neurons to astrocytes) and in that of [4,5-^{13}C]glutamate and glutamine (suggesting normal transfer of glutamine from astrocytes to neurons). Normal transfer of glutamine from astrocytes to GABAergic neurons is suggested by the concurrent increase in percentage enrichment of [1,2-^{13}C]GABA and [4,5-^{13}C]glutamine. The increased percentage enrichment of [4,5-^{13}C]glutamate, [4-^{13}C]glutamine and [1,2-^{13}C]GABA therefore probably reflected the increased ^{13}C labeling of their respective precursors.

Different Metabolic States in Hippocampus and Cortex

The fact that two distinct metabolic states were evident as a consequence of tau hyperphosphorylation in hippocampus and cerebral cortex may be related to the fact that human mutated tau is present to a larger extent in hippocampus than in neocortex in pR5 mice at age 3 months.[20] Thus, our results may indicate that the metabolic consequences can differ according to the level of hyperphosphorylated tau and may possibly represent different stages of the metabolic response to tau pathology. Alternatively, this difference may reflect selective vulnerability,[38] which has been shown for the hippocampus in FTD.[39] The reason for the apparent upregulation of cortical metabolism at this age remains unclear and appears contradictory to the reports on hypometabolism in AD and FTD patients[12,15] and the severe mitochondrial dysfunction that has been demonstrated in pR5 mice at a later age.[29] It is possible that these early changes in cortex in the present study may reflect compensatory mechanisms, which indeed appear to occur in response to the expression of the P301L mutation in tau. At age 1 to 2 months, before the onset of marked tau hyperphosphorylation, other lines of mice that also express the P301L mutation display paradoxical increases in long-term potentiation of synapses in dentate gyrus and in dendritic spine maturation in addition to improved cognitive performance compared with controls.[34,40] The downregulation of several metabolism-related proteins and reduced complex I activity as measured in the whole brain at the ages 8.5 to 12 months suggests that metabolic dysfunction occurs in pR5 mice with increased aggregation of tau. However, mitochondrial respiration, ATP production, and oxidative status as measured in one hemisphere are preserved until advanced age and massive NFT deposition.[29] Studies in patients with mild FTD demonstrate that decreased glucose metabolism is restricted to distinct cortical regions whereas other cortical regions remain unaffected.[14] Local variations in the metabolic pattern obtained in cortex in the present study cannot be excluded, as the use of the whole cortex may have masked regional metabolic differences in more spatially confined regions. In the hippocampus, however, a mutated tau-dependent metabolic deterioration appears to occur already at the age of 3 months in P301L tau-expressing pR5 mice.

Overall, we revealed that astrocytes as well as glutamatergic and GABAergic neurons in the cortex of pR5 mice were in a hypermetabolic state, whereas in the hippocampus, where expression levels of mutant human tau are the highest, glutamate homeostasis was impaired.

DISCLOSURE/CONFLICT OF INTEREST

The authors declare no conflict of interest.

ACKNOWLEDGEMENTS

The technical assistance of Lars G Evje and Mohammed A Kashem is gratefully acknowledged. We thank the Norwegian Health Association (Dementia) and the Department of Neuroscience DMF/NTNU for financial support.

REFERENCES

1 Rizzu P, Joosse M, Ravid R, Hoogeveen A, Kamphorst W, van Swieten JC *et al.* Mutation-dependent aggregation of tau protein and its selective depletion from the soluble fraction in brain of P301L FTDP-17 patients. *Hum Mol Genet* 2000; **9**: 3075–3082.

2 Goedert M, Wischik CM, Crowther RA, Walker JE, Klug A. Cloning and sequencing of the cDNA encoding a core protein of the paired helical filament of Alzheimer disease: identification as the microtubule-associated protein tau. *Proc Natl Acad Sci USA* 1988; **85**: 4051–4055.

3 Bramblett GT, Goedert M, Jakes R, Merrick SE, Trojanowski JQ, Lee VM. Abnormal tau phosphorylation at Ser396 in Alzheimer's disease recapitulates development and contributes to reduced microtubule binding. *Neuron* 1993; **10**: 1089–1099.

4 Goedert M, Spillantini MG, Jakes R, Crowther RA, Vanmechelen E, Probst A *et al.* Molecular dissection of the paired helical filament. *Neurobiol Aging* 1995; **16**: 325–334.

5 Götz J, Ittner LM, Kins S. Do axonal defects in tau and amyloid precursor protein transgenic animals model axonopathy in Alzheimer's disease? *J Neurochem* 2006; **98**: 993–1006.

6 Buee L, Bussiere T, Buee-Scherrer V, Delacourte A, Hof PR. Tau protein isoforms, phosphorylation and role in neurodegenerative disorders. *Brain Res Brain Res Rev* 2000; **33**: 95–130.

7 Hutton M, Lendon CL, Rizzu P, Baker M, Froelich S, Houlden H *et al.* Association of missense and 5′-splice-site mutations in tau with the inherited dementia FTDP-17. *Nature* 1998; **393**: 702–705.

8 Poorkaj P, Bird TD, Wijsman E, Nemens E, Garruto RM, Anderson L *et al.* Tau is a candidate gene for chromosome 17 frontotemporal dementia. *Ann Neurol* 1998; **43**: 815–825.

9 Spillantini MG, Murrell JR, Goedert M, Farlow MR, Klug A, Ghetti B. Mutation in the tau gene in familial multiple system tauopathy with presenile dementia. *Proc Natl Acad Sci USA* 1998; **95**: 7737–7741.

10 Spillantini MG, Van Swieten JC, Goedert M. Tau gene mutations in frontotemporal dementia and parkinsonism linked to chromosome 17 (FTDP-17). *Neurogenetics* 2000; **2**: 193–205.

11 Ishii K, Sakamoto S, Sasaki M, Kitagaki H, Yamaji S, Hashimoto M *et al.* Cerebral glucose metabolism in patients with frontotemporal dementia. *J Nucl Med* 1998; **39**: 1875–1878.

12 Kanda T, Ishii K, Uemura T, Miyamoto N, Yoshikawa T, Kono AK *et al.* Comparison of grey matter and metabolic reductions in frontotemporal dementia using FDG-PET and voxel-based morphometric MR studies. *Eur J Nucl Med Mol Imaging* 2008; **35**: 2227–2234.

13 Jeong Y, Cho SS, Park JM, Kang SJ, Lee JS, Kang E *et al.* 18F-FDG PET findings in frontotemporal dementia: an SPM analysis of 29 patients. *J Nucl Med* 2005; **46**: 233–239.

14 Diehl-Schmid J, Grimmer T, Drzezga A, Bornschein S, Riemenschneider M, Forstl H *et al.* Decline of cerebral glucose metabolism in frontotemporal dementia: a longitudinal 18F-FDG-PET-study. *Neurobiol Aging* 2007; **28**: 42–50.

15 Mosconi L, Pupi A, De Leon MJ. Brain glucose hypometabolism and oxidative stress in preclinical Alzheimer's disease. *Ann NY Acad Sci* 2008; **1147**: 180–195.

16 Fellgiebel A, Siessmeier T, Scheurich A, Winterer G, Bartenstein P, Schmidt LG *et al.* Association of elevated phospho-tau levels with Alzheimer-typical 18F-fluoro-2-deoxy-D-glucose positron emission tomography findings in patients with mild cognitive impairment. *Biol Psychiatry* 2004; **56**: 279–283.

17 Kantarci K, Boeve BF, Wszolek ZK, Rademakers R, Whitwell JL, Baker MC *et al.* MRS in presymptomatic MAPT mutation carriers: a potential biomarker for tau-mediated pathology. *Neurology* 2010; **75**: 771–778.

18 Bak LK, Schousboe A, Waagepetersen HS. The glutamate/GABA-glutamine cycle: aspects of transport, neurotransmitter homeostasis and ammonia transfer. *J Neurochem* 2006; **98**: 641–653.

19 Götz J, Chen F, Barmettler R, Nitsch RM. Tau filament formation in transgenic mice expressing P301L tau. *J Biol Chem* 2001; **276**: 529–534.

20 Deters N, Ittner LM, Gotz J. Divergent phosphorylation pattern of tau in P301L tau transgenic mice. *Eur J Neurosci* 2008; **28**: 137–147.

21 Qu H, Haberg A, Haraldseth O, Unsgard G, Sonnewald U. (13)C MR spectroscopy study of lactate as substrate for rat brain. *Dev Neurosci* 2000; **22**: 429–436.

22 Hassel B, Sonnewald U, Fonnum F. Glial-neuronal interactions as studied by cerebral metabolism of [2-13C]acetate and [1-13C]glucose: an *ex vivo* 13C NMR spectroscopic study. *J Neurochem* 1995; **64**: 2773–2782.

23 Sonnewald U, Westergaard N, Schousboe A, Svendsen JS, Unsgard G, Petersen SB. Direct demonstration by [13C]NMR spectroscopy that glutamine from astrocytes is a precursor for GABA synthesis in neurons. *Neurochem Int* 1993; **22**: 19–29.

24 Taylor A, McLean M, Morris P, Bachelard H. Approaches to studies on neuronal/glial relationships by 13C-MRS analysis. *Dev Neurosci* 1996; **18**: 434–442.

25 Haberg A, Sonnewald U, Hammer J, Melø TM, Eloqayli H. 13C NMR Spectroscopy as a Tool in Neurobiology. In: Choi IY, Gruetter R (eds). *Neural Metabolism In Vivo*. pp 221–253 (Springer: New York, 2012).

26 Kondziella D, Brenner E, Eyjolfsson EM, Markinhuhta KR, Carlsson ML, Sonnewald U. Glial-neuronal interactions are impaired in the schizophrenia model of repeated MK801 exposure. *Neuropsychopharmacology* 2006; **31**: 1880–1887.

27 Götz J, Gladbach A, Pennanen L, van Eersel J, Schild A, David D *et al.* Animal models reveal role for tau phosphorylation in human disease. *Biochim Biophys Acta* 2010; **1802**: 860–871.

28 Mosconi L, Tsui WH, De Santi S, Li J, Rusinek H, Convit A *et al.* Reduced hippocampal metabolism in MCI and AD: automated FDG-PET image analysis. *Neurology* 2005; **64**: 1860–1867.

29 David DC, Hauptmann S, Scherping I, Schuessel K, Keil U, Rizzu P *et al.* Proteomic and functional analyses reveal a mitochondrial dysfunction in P301L tau transgenic mice. *J Biol Chem* 2005; **280**: 23802–23814.
30 Ernst T, Chang L, Melchor R, Mehringer CM. Frontotemporal dementia and early Alzheimer disease: differentiation with frontal lobe H-1 MR spectroscopy. *Radiology* 1997; **203**: 829–836.
31 Rupsingh R, Borrie M, Smith M, Wells JL, Bartha R. Reduced hippocampal glutamate in Alzheimer disease. *Neurobiol Aging* 2011; **32**: 802–810.
32 Nilsen LH, Melo TM, Saether O, Witter MP, Sonnewald U. Altered neurochemical profile in the McGill-R-Thy1-APP rat model of Alzheimer's disease: a longitudinal *in vivo* (1) H MRS study. *J Neurochem* 2012; **123**: 532–541.
33 Haris M, Nath K, Cai K, Singh A, Crescenzi R, Kogan F *et al.* Imaging of glutamate neurotransmitter alterations in Alzheimer's disease. *NMR Biomed* 2012; doi: 10.1002/nbm.2875 [e-pub ahead of print].
34 Boekhoorn K, Terwel D, Biemans B, Borghgraef P, Wiegert O, Ramakers GJ *et al.* Improved long-term potentiation and memory in young tau-P301L transgenic mice before onset of hyperphosphorylation and tauopathy. *J Neurosci* 2006; **26**: 3514–3523.
35 Ittner LM, Ke YD, Gotz J. Phosphorylated Tau interacts with c-Jun N-terminal kinase-interacting protein 1 (JIP1) in Alzheimer disease. *J Biol Chem* 2009; **284**: 20909–20916.
36 Lei H, Duarte JM, Mlynarik V, Python A, Gruetter R. Deep thiopental anesthesia alters steady-state glucose homeostasis but not the neurochemical profile of rat cortex. *J Neurosci Res* 2010; **88**: 413–419.
37 Hassel B, Bachelard H, Jones P, Fonnum F, Sonnewald U. Trafficking of amino acids between neurons and glia *in vivo*. Effects of inhibition of glial metabolism by fluoroacetate. *J Cereb Blood Flow Metab* 1997; **17**: 1230–1238.
38 Götz J, Schonrock N, Vissel B, Ittner LM. Alzheimer's disease selective vulnerability and modeling in transgenic mice. *J Alzheimers Dis* 2009; **18**: 243–251.
39 Laakso MP, Frisoni GB, Kononen M, Mikkonen M, Beltramello A, Geroldi C *et al.* Hippocampus and entorhinal cortex in frontotemporal dementia and Alzheimer's disease: a morphometric MRI study. *Biol Psychiatry* 2000; **47**: 1056–1063.
40 Kremer A, Maurin H, Demedts D, Devijver H, Borghgraef P, Van Leuven F. Early improved and late defective cognition is reflected by dendritic spines in Tau.P301L mice. *J Neurosci* 2011; **31**: 18036–18047.